Contemporary Mathematics
http://ojs.wiserpub.com/index.php/CM/

Research Article

Modeling Rabies Dynamics: The Impact of Vaccination and Infectious Immigrants on Public Health

Hazrat Younas[1], Imtiaz Ahmad[1], Nigar Ali[1], Ihtisham Ul Haq[1*], Mohammed Daher Albalwi[2], Shah Muhammad[3], Mohammad Shuaib[4]

[1]Department of Mathematics, University of Malakand, Chakdara Dir(L), 18000, Khyber Pakhtunkhwa, Pakistan
[2]Yanbu Industrial College, The Royal Commission for Jubail and Yanbu, 30436, Saudi Arabia
[3]Department of Mathematics, College of Science, King Saud University, Riyadh, Saudi Arabia
[4]Department of Mathematics, Lovely Professional University, Phagwara, Punjab, India
E-mail: ihtisham0095@gmail.com

Received: 23 May 2024; **Revised:** 5 July 2024; **Accepted:** 24 July 2024

Abstract: Public health is still seriously threatened by rabies in many parts of the world, particularly in poorer nations. In order to address this issue, this work suggests an equation describing the mechanisms of rabies transmission between animals, taking into account infectious immigrants and vaccination as possible preventive measures. The next-generation matrix (NGM) Method method was used to calculate the effective reproduction number (R_0). Using the Routh-Hurwitz Criterion, a disease-free equilibrium point (DFE) was discovered and It was demonstrated to have local asymptotic stability if $(R_0 < 1)$, and unstable in every other case. Additionally, DFE was discovered to be quadratic Lyapunov stable and globally asymptotically stable. Additionally, the model parameters' sensitivity analysis on the (R_0) was carried out using the central manifold theory for the bifurcation analysis, and the analysis's normalized forward sensitivity index method. MATLAB software was utilized to do numerical analysis for simulation analysis. The findings of the simulated data showed that a higher vaccination rate and fewer infectious immigrants would slow the development of the decline, as shown visually.

***Keywords*:** SEV IR mathematical model, rabies, stability analysis, bifurcation, numerical simulation

MSC: 92D30, 37N25, 34C60

Abbreviation

RIG	Rabies Immune Globulin
CDC	Control of Diseases Centers
NGM	Next-Generation Matrix
PEP	Post-Exposure Prophylaxis
SEV IR	Susceptible Exposed Vaccinated Infected and Recovered

DOI: https://doi.org/10.37256/cm.5320245010

1. Introduction

Humans and other mammals are susceptible to the zoonotic disease rabies, which is caused by a rabies virus. It belongs to the genus Lyssavirus and family Rhabdoviridae [1, 2]. Since the virus is found in saliva, the most common method of transmission is through an animal's bite [3]. Dogs are the primary mammals that transmit the rabies virus from other animals to humans, along with bats, skunks, raccoons, foxes, and cats [4]. Peripheral nerves allow rabies to penetrate the central nervous system. The virus causes encephalitis, which results in severe neurological symptoms that worsen over time, such as paralysis of the muscles, anxiety, and aberrant neurological signs [5, 6]. Rabies continues to be a major global health concern, accounting for over 59,000 deaths annually, a large majority of which occur in Africa and Asia [7]. It is true that rabies is a deadly disease, and that once infected, recovery is quite unlikely. In extremely rare instances, rabies virus infections can be recovered from but result in serious neurological impairments.

Since the illness may cause the patient to suffer from severe physical or mental disability, this is not a true cure in the traditional sense. There have been reported cases of people surviving with no significant neurological aftereffects, despite the fact that they are incredibly rare. The research is incredibly weak when it comes to assertions that an infected animal with rabies can survive. Although there have been fewer occurrences of rabies in some areas, the disease is still widespread, especially particularly sub-Saharan Africa and Southeast Asia, where access is restricted to inexpensive livestock immunizations and prompt post-exposure prophylaxis [8]. Despite the fact that vaccinations can prevent dog rabies, tens of thousands of people die from the disease annually in low- and middle-income nations [9, 10]. Even if exposed to the virus, rabies is extremely uncommon to strike someone who has received the recommended vaccination against the disease. Antibodies that guard against the virus are produced as a result of receiving a rabies vaccination. Before the rabies virus can spread and infect people, these antibodies aid in neutralizing it. Regardless of immunization status, PEP is recommended following possible exposure to rabies. In order to defend against the virus, PEP entails giving rabies vaccines and, in certain situations, RIG. Preventive and CDC state that people who receive a full pre-exposure vaccination are thought to have long-term immunity and typically do not need booster doses unless they work in a field where exposure to rabies virus is constant, such as veterinary medicine or laboratory work handling samples of the virus. Depending on the environmental circumstances, domestic or wild animals can infect humans with rabies, underscoring the significance of caution and preventive measures [11–14].

Complex dynamics including population density, wildlife populations, and vaccination campaigns all have an impact on the dynamics of rabies transmission. The dynamics of illness, particularly the spread of rabies, have been better understood thanks to mathematical modeling. A number of disease modeling-related topics, including asymptotic stability, media effect, contagion, and treatment techniques, have been the subject of recent research [15, 16]. Specifically, several mathematical models have analyzed the dynamics of rabies transmission and proposed mitigation and control strategies. However, externally imported illnesses are often overlooked in traditional models, despite the fact that they might significantly affect the transmission [17].

Various mathematical models have recently analyzed the dynamics of rabies transmission and have suggested control for preventing the disease. However, the traditional models, mostly avoid the major possibility of externally imported infections that mostly contributes and had a substantial impact on the spread of the disease of rabies in natural reservoirs. The current paper addresses this limitation by including the effects of infected immigrants, by combining the Routh-Hurwitz criterion, a quadratic Lyapunov function, and a NGM approach. These methods shall meet our goal for enhancing the model accuracy, dependability, and practicality. Taking in to account the WHO rules, we shall present a fresh perspective on modeling the dynamics of animal rabies while maintaining the credibility of the given sources. This approach shall also concentrate on the primary fact to dispel any misconceptions that appears in literature regarding recovery from rabies, that is, often recorded and recognized almost fatal.

2. Formulation of mathematical

A nonlinear mathematical model comprising of five compartments namely, Susceptible, Vaccinated, Exposed, Infected, and Recovered shall be considered. The model shall aim to look into and evaluate how the disease's dynamics

relate the infectious animal immigrants and the animal rabies. Receptive Animals in $S(t)$ are those that are not infected but could become infected following meaningful interaction with contaminated animals; exposed animals Animals with rabies infection but no contagious disease are represented by $E(t)$; these are vaccinated animals. Vaccinated animals from the susceptible animal population are denoted by $V(t)$; these animals are infected. The animals $I(t)$ are those that are communicable due to having received the rabies virus; animals that have been retrieved in $R(t)$ have recovered from rabies infections by either treatment or a natural immunological response.

Birth rate and immigration at π are believed to be the sources of hiring into the class $S(t)$ that is vulnerable. Interaction between the infected $I(t)$ and susceptible $S(t)$ causes infections at a rate of β. At a rate of θ, only vulnerable animals in the population $S(t)$ receive vaccinations, moving on to the vaccinated class $V(t)$. The vaccine efficacy is represented by the parameter ε, since vaccinations may not always be 100% successful. Animals lose immunity and revert to being susceptible at a pace τ. After being exposed to the disease virus, animals move up to the infected class $I(t)$ and become infectious at a rate of σ. Immigration causes the proportion π_i to enter the infected class $I(t)$. The animals that have recovered experience a decline in immunity and revert to the susceptible class $S(t)$; rate η. Both contribute to the decline in the animal population. Figure 1 represents the flow-chart of the proposed model.

$$\begin{aligned}
\frac{dS}{dt} &= \pi + \eta R + \tau V - (\beta I + \theta + \mu)S, \\
\frac{dE}{dt} &= \beta SI + (1-\varepsilon)\beta VI - (\alpha_1 + \alpha_2 + \delta + \mu)E, \\
\frac{dI}{dt} &= \pi_i + \delta E - (\mu + \mu_1)I, \\
\frac{dV}{dt} &= \alpha_1 E + \theta S - (\tau + \mu + (1-\varepsilon)\beta I)V, \\
\frac{dR}{dt} &= \alpha_2 E - (\mu + \eta)R.
\end{aligned} \tag{1}$$

Initial conditions are given in the Figure 1:

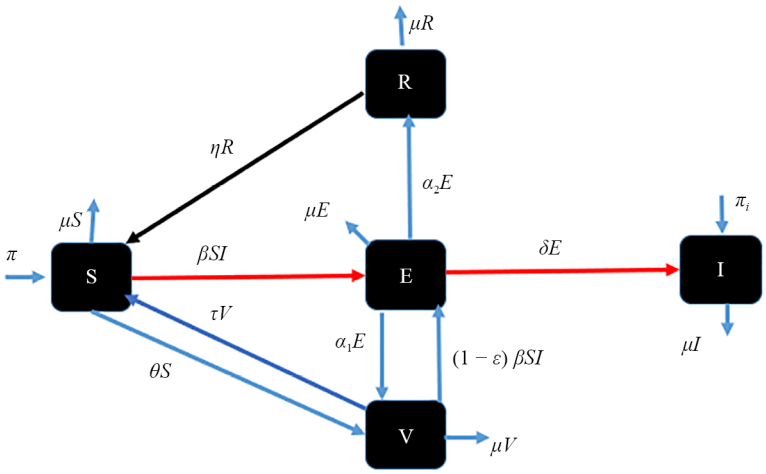

Figure 1. Flow-chart of the proposed model

$$S(0) > 0, \quad E(0) \geq 0, \quad I(0) \geq 0, \quad V(0) \geq 0, \quad R(0) \geq 0, \tag{2}$$

3. The basics qualitative properties of the model (1)

The rabies model presented in (1) is only mathematically and physiologically significant if and when all of the model solutions (State variables) are limited in the invariant area and non-negative.

$$\Omega = \left\{ (S,\, E,\, I,\, V,\, R) \in \mathbb{R}^5_+ \,\middle|\, N \leq \frac{\pi + \pi_i}{\mu} \right\}$$

3.1 *Positivity of the model solution*

Theorem 1 [18] Let us give the initial data in Eq.(2) then the solutions $S(t), E(t), I(t), V(t), R(t)$, of the rabies model are non-negative for all times $t > 0$.

Proof. Let us consider $S(0) > 0, E(0) > 0, I(0) > 0, V(0) > 0, R(0) > 0$, then for all $t > 0$. We have to show that $S(0) > 0, E(0) > 0, I(0) > 0, V(0) > 0, R(0) > 0$.

Define: $\omega = \sup\{S(0) > 0,\, E(0) > 0,\, I(0) > 0,\, V(0) > 0,\, R(0) > 0\}$.

We can now argue that $\omega > 0$ since all of the state variables in model (1) are positive and continuous. If $\omega = +\infty$, then the non-negativity holds. But, if $0 < \omega < +\infty$, we will have $S(\omega) = 0$, or $E(\omega) = 0$, or $I(\omega) = 0$, or $V(\omega) > 0$, or $R(\omega) > 0$. We have found the constant value via integrating.

$$S(\omega) = M_1 S(0) + M_1 \int_0^{\omega} \exp\left(\int (\pi + (\mu + \theta)(t))\, dt \right) (\tau V + \gamma R - \beta IS) dt > 0$$

Where $M_1 = \exp\left(-\left(\pi t + \int_0^{\omega} (\mu(t) + \theta(t)) dt \right) \right) > 0$.

And from the meaning of ω, the solution of $S(0) > 0$, $E(0) > 0$, $I(0) > 0$, $S(\omega) \neq 0$. Thus following the same procedure for $\omega = +\infty$, all the solutions of the model (1) are non-negative.

3.2 *Disease free equilibrium point (DFE)*

Equation (1)'s equilibrium solution may be found by setting the derivatives to zero and working through the algebraic equations [19]. An example of an equilibrium solution for an illness is as follows:

By setting $E(t) = I(t) = R(t) = 0$ in each equation, DFE can be found. Thus, DFE is provided by:

$$E_0 = \left(S^0,\, E^0,\, V^0,\, I^0,\, R^0,\right) = \left(\frac{\phi\mu(\theta + \phi + \mu) + (\theta\tau\phi)}{(\theta + \mu)\mu(\theta + \tau + \mu)}, \quad 0, \quad \frac{\pi\theta}{\mu(\theta + \tau + \mu)}, \quad 0, \quad 0 \right).$$

3.3 *Endemic equilibrium point*

The situation where $I \neq 0$ is represented by a second equilibrium solution that is acquired by the solution of the algebraic equation system [19]. This solution, which goes by the name "endemic equilibrium solution," is as follows:

$$\begin{cases} S^* = \dfrac{\phi\mu(\theta+\phi+\mu)+(\theta\tau\phi)}{(\theta+\mu)\mu(\theta+\tau+\mu)}, \\ E^* = \dfrac{(\mu+\mu_1)-\phi}{\delta}, \\ I^* = \dfrac{A_1+\theta\tau\theta\delta}{A_2-\theta(1-\varepsilon)\beta\theta\phi(\tau+\mu)(\theta+\mu)+\theta\tau\theta\delta}, \\ V^* = \dfrac{\pi\theta}{\mu(\theta+\tau+\mu)}, \\ R^* = \dfrac{\alpha_2(\mu+\mu_1)-\phi}{\delta(\mu+\eta)} \end{cases}$$

Where: $A_1 = \phi(\alpha_1+\alpha_2+\delta+\mu)\mu(\theta+\tau+\mu)(\tau+\mu)+\theta\tau\theta\delta$, $A_2 = (\alpha_1+\alpha_2+\delta+\mu)+(\mu+\mu_1)$.

4. Basic reproductive number

In epidemiology, the Basic Reproductive Number is a fundamental concept. or quantifies the ability for an infectious illness to spread. It shows how many secondary infections, on average, an infected person in a vulnerable population causes. Stated differently, it measures the degree to which an illness can proliferate among a group of people. If $R_0 > 1$, then multiple new infections are being caused by each current illness, suggesting that the disease will probably spread across the population.

If $R_0 < 1$, then less than one new infection is being caused by each current illness, indicating that the disease will probably eventually become extinct in the population. We now apply the R_0 method as follows to determine R_0:

$$F = \begin{pmatrix} \beta SI+(1-\varepsilon)\beta VI \\ 0 \end{pmatrix}, \quad F^* = \begin{pmatrix} 0 & \beta S^*+(1-\varepsilon)\beta V^* \\ 0 & 0 \end{pmatrix}$$

$$V = \begin{pmatrix} (\alpha_1+\alpha_2+\delta+\mu)E \\ (\mu+\mu_1)I-\delta E-\pi_i \end{pmatrix}, \quad V^* = \begin{pmatrix} \alpha_1+\alpha_2+\delta+\mu & 0 \\ -\delta & \mu+\mu_1 \end{pmatrix}$$

The inverse of V is:

$$V^{-1} = \frac{\text{adj}(V)}{|V|} = \begin{pmatrix} \dfrac{1}{\alpha_1+\alpha_2+\delta+\mu} & 0 \\ \dfrac{\delta}{(\alpha_1+\alpha_2+\delta+\mu)(\mu+\mu_1)} & \dfrac{1}{\mu+\mu_1} \end{pmatrix}$$

We then find F^*V^{-1}:

$$F^{*}V^{-1} = \begin{pmatrix} \dfrac{\beta\pi((\tau+\mu)+(1-\varepsilon)\theta)}{(\alpha_1+\alpha_2+\delta+\mu)(\mu+\tau)(\mu+\theta)(\mu+\mu_1)} & \dfrac{\beta\pi((\tau+\mu)+(1-\varepsilon)\theta)}{(\mu+\tau)(\mu+\theta)(\mu+\mu_1)} \\ 0 & 0 \end{pmatrix}$$

The dominant eigenvalue of this next-generation matrix is called the basic reproduction number R_0, which is:

$$R_0 = \frac{\beta\pi((\tau+\mu)+(1-\varepsilon)\theta)}{(\alpha_1+\alpha_2+\delta+\mu)(\mu+\tau)(\mu+\theta)(\mu+\mu_1)}$$

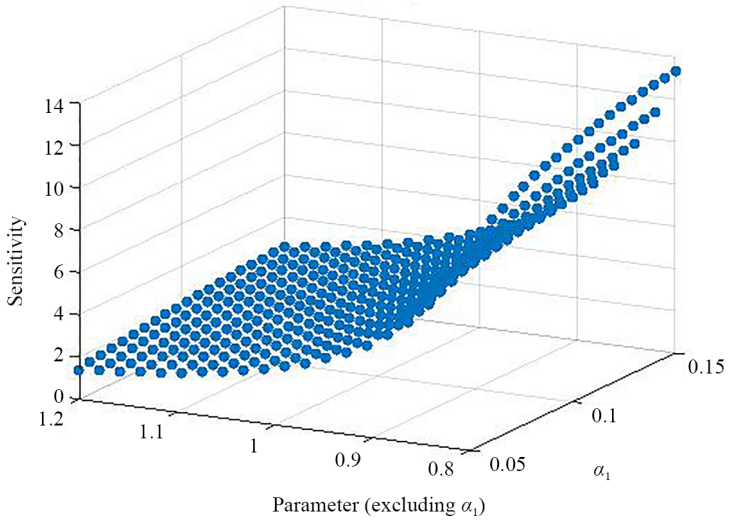

Figure 2. Sensitivity analysis of R_0 to α_1 and other parameters

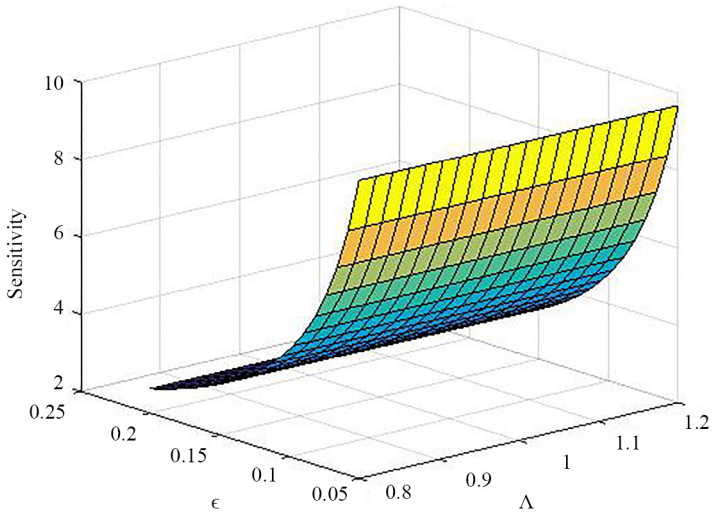

Figure 3. Sensitivity analysis of R_0 to Λ and ε

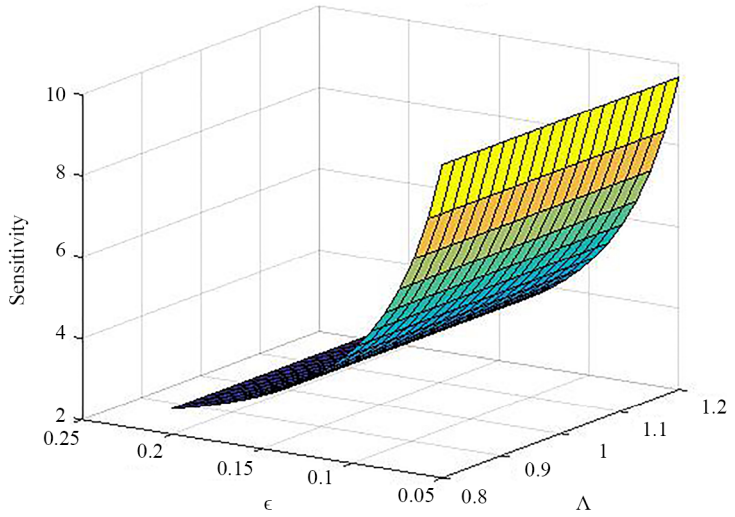

Figure 4. Sensitivity analysis of R_0 to γ

Figures 2, 3, and 4 represent the effect of different parameters on R_0.

5. Sensitivity analysis

The model parameters and their effects on the effective reproduction number are discussed in the sensitivity analysis. R_0, as well as the transmission of the disease. Sensitivity indices can be used to quantify each parameter's contribution to the spread of a disease, and model analysis can be used to evaluate how robustly predictions are made to parameter values [19].

Sensitivity analysis tells the researcher which parameters require greater numerical attention and which initial conditions and parameters affect the model output. The variable R_0,'s normalized forward sensitivity index is dependent on the differentiability of a parameter p, which has the following definition:

Where $X_p^{R_0} = \frac{\partial R_0}{\partial p} \times \frac{p}{R_0}$, symbolize the sensitivity index, and the effective reproduction number's parameter is k. For instance, The number of effective reproductions is increased. by increasing the value of Table 1, which is positive managing; the more a parameter's value effects the reverse, or the number of effective reproductions. The parameter index is presented as Table 1. To see refer to table for the indices of the remaining parameters.

$$X_p^{R_0} = \frac{\partial R_0}{\partial p} \times \frac{p}{R_0},$$

$$p = \{\beta,\ \pi,\ \tau,\ \mu,\ \varepsilon,\ \theta,\ \alpha_1,\ \alpha_2,\ \delta,\ \mu_1\}$$

$$
\begin{cases}
X_{\beta}^{R_0} = \dfrac{\partial R_0}{\partial \beta} \times \dfrac{\beta}{R_0} = 1 \\
X_{\pi}^{R_0} = \dfrac{\partial R_0}{\partial \pi} \times \dfrac{\pi}{R_0} = 1, \\
X_{\tau}^{R_0} = \dfrac{\partial R_0}{\partial \tau} \times \dfrac{\tau}{R_0} = \dfrac{\tau(\alpha_1+\alpha_2+\delta+\mu)(\mu+\tau)(\mu+\theta)(\mu+\mu_1)}{\beta\pi((\tau+\mu)+(1-\varepsilon)\theta)}, \\
X_{\mu}^{R_0} = \dfrac{\partial R_0}{\partial \mu} \times \dfrac{\mu}{R_0} = \dfrac{(\alpha_1+\alpha_2+\delta+\mu)(\mu+\tau)(\mu+\theta)(\mu+\mu_1)}{\beta\pi((\tau+\mu)+(1-\varepsilon)\theta)} \times \left(\dfrac{4\mu^3+3(\tau+\theta+\mu_1)\mu^2+2(\tau\theta+\tau\mu_1+\theta\mu_1)\mu}{1}\right), \\
X_{\varepsilon}^{R_0} = \dfrac{\partial R_0}{\partial \varepsilon} \times \dfrac{\varepsilon}{R_0} \dfrac{(\alpha_1+\alpha_2+\delta+\mu)(\mu+\tau)(\mu+\theta)(\mu+\mu_1)}{\beta\pi((\tau+\mu)+(1-\varepsilon)\theta)} \times \left(\dfrac{4\varepsilon\mu^3+3\varepsilon(\tau+\theta+\mu_1)\mu^2+2\varepsilon(\tau\theta+\tau\mu_1+\theta\mu_1)\mu}{1}\right), \\
X_{\alpha_1}^{R_0} = \dfrac{\partial R_0}{\partial \alpha_1} \times \dfrac{\alpha_1}{R_0} - \dfrac{\alpha_1(\alpha_1+\alpha_2+\delta+\mu)(\mu+\tau)(\mu+\theta)(\mu+\mu_1)}{(\tau+\mu)+(1-\varepsilon)\theta}, \\
X_{\alpha_2}^{R_0} = \dfrac{\partial R_0}{\partial \alpha_2} \times \dfrac{\alpha_2}{R_0} - \dfrac{\alpha_2(\alpha_1+\alpha_2+\delta+\mu)(\mu+\tau)(\mu+\theta)(\mu+\mu_1)}{(\tau+\mu)+(1-\varepsilon)\theta}, \\
X_{\delta}^{R_0} = \dfrac{\partial R_0}{\partial \delta} \times \dfrac{\delta}{R_0} - \dfrac{\delta(\alpha_1+\alpha_2+\delta+\mu)(\mu+\tau)(\mu+\theta)(\mu+\mu_1)}{(\tau+\mu)+(1-\varepsilon)\theta}, \\
X_{\mu_1}^{R_0} = \dfrac{\partial R_0}{\partial \mu_1} \times \dfrac{\mu_1}{R_0} \dfrac{\mu_1(\alpha_1+\alpha_2+\delta+\mu)(\mu+\tau)(\mu+\theta)(\mu+\mu_1)}{(\tau+\mu)+(1-\varepsilon)\theta}
\end{cases}
$$

Table 1. Parameter values and sensitivity index

Parameters	Value (per day)	Source	Sensitivity index
μ	0.1	[20]	0.3
α_1	0.1	Assume	-0.08
α_2	0.1	Assume	-0.9
δ	0.1	Assume	-1.4
τ	0.1	[20]	1.5
ε	0.1	Assume	0.2
β	0.2	[20]	1
μ_1	0.05	[20]	0.07
π	0.1	[20]	1
θ	0.1	[20]	0.1

6. Local stability of disease free equilibrium

Theorem 2 In the model system (1), the disease-free equilibrium point E^0 is locally asymptotically stable if $R_0 < 1$, and unstable otherwise.

Proof. Applying the Routh Hurwitz stability criteria of the rubies model described in eq. (1) at the illness-free equilibrium point E^0 yields the following results:the local stability of the illness of the disease-free equilibrium point of model (1) is assessed by,

$$\begin{bmatrix} -(\mu+\theta) & \theta & \beta^* S^* & \tau & \eta \\ 0 & -(u+\alpha_1+\alpha_2) & \beta^* S^* & 0 & 0 \\ 0 & \delta & -(u+u_1) & 0 & 0 \\ 0 & \alpha_1 & 0 & (u+\tau) & 0 \\ 0 & \alpha_2 & 0 & 0 & -(u+\eta) \end{bmatrix}$$

Next, the matching characteristics of the jecobian matrix $J(E^0)$ is given by,

$$\begin{bmatrix} -(\mu+\theta)-\lambda & \theta & \beta^* S^* & \tau & \eta \\ 0 & -(u+\alpha_1+\alpha_2)-\lambda & \beta^* S^* & 0 & 0 \\ 0 & \delta & -(u+u_1)-\lambda & 0 & 0 \\ 0 & \alpha_1 & 0 & -(u+\tau)-\lambda & 0 \\ 0 & \alpha_2 & 0 & 0 & -(u+\eta)-\lambda \end{bmatrix}$$

$$\lambda_1 = -(u+r),\ \lambda_2 = -(u+t),\ \lambda_3 = -(u+t),$$

The above matrix is reduced

$$(J(E^0) - \lambda I) = \begin{bmatrix} -(a_1+a_2+\delta)-\lambda & BS^* \\ \delta & -(u_1+u_2)-\lambda \end{bmatrix} = 0,$$

$$((u+a_1+a_2+\delta)-\lambda)((u+u_1)-\delta BS^*) = 0,$$

$$\lambda^2 + \lambda(\theta u - \alpha_1 + \alpha_2 - \delta - u_1 + (u^2 + uu_1 + \alpha_1 u_1 + \alpha_2 u + \alpha_2 u_1 - BS^*)) = 0,$$

Here

$$B_1 = (a_1 - 2u - u - \delta - u_1)$$

$$B_2 = (u^2 + uu_1 + a_1 u + a_2 u + a_2 u_1 - \delta BS^*)$$

$$\lambda^2 + \lambda B_1 + B_2 = 0,$$

Whenver $R_0 < 1$, if the initial size of the model is given (1), is in the basin of attraction of the disease-free equation point (E^0), It may be inferred that the model's disease-free equilibrium point (1) exhibits local asymptotic stability. □

7. Global stability of the endemic equilibrium point

Utilizing Vargas-De-Leon's Lyapunov function [21], The point at which the endemic equilibrium is globally stable E^* was evaluated. If $\frac{dV}{dt} < 0$, the Lyapunov function $V(x)$ is considered to be asymptotically globally stable at the point where it exists.

Theorem 3 For the given model system, the rabies epidemic has a unique endemic equilibrium point (E^*), which is globally asymptotically stable if $R_0 > 1$ and unstable otherwise.

Proof. Consider the quadratic Lyapunov function

$$v(y) = \frac{1}{2}\sum_{i=1}^{n}(y_i - y_i^*)^2,$$

where y_i is the population of the i-th compartment and y_i^* is its endemic equilibrium value.

This function is positive definite for the model system.

The Lyapunov function for the rabies model system can be expressed as:

$$v = \frac{1}{2}\left((S-S^*)^2 + (E-E^*)^2 + (I-I^*)^2 + (V-V^*)^2 + (R-R^*)^2\right).$$

Taking the time derivative of v, we get:

$$\frac{dv}{dt} = (S-S^*)\frac{dS}{dt} + (E-E^*)\frac{dE}{dt} + (I-I^*)\frac{dI}{dt} + (V-V^*)\frac{dV}{dt} + (R-R^*)\frac{dR}{dt}.$$

Using the model equations, we substitute

$$\frac{dS}{dt}, \frac{dE}{dt}, \frac{dI}{dt}, \frac{dV}{dt}, \text{ and } \frac{dR}{dt}:$$

$$\frac{dv}{dt} = ((S+E+I+V+R) - (S^*+E^*+I^*+V^*+R^*))(\pi + \pi_i - \mu I - \mu N).$$

At equilibrium, we have:

$$\pi + \pi_i - \mu I - \mu(S^*+E^*+I^*+V^*+R^*) = 0.$$

This implies:

$$(S^*+E^*+I^*+V^*+R^*) = \frac{\pi + \pi_i - \mu I^*}{\mu}.$$

Substituting this into the derivative, we get:

$$\frac{dv}{dt} = -\mu \left(N(t) - \frac{\pi + \pi_i - \mu I^*}{\mu} \right)^2.$$

Since $\mu > 0$, it follows that:

$$\frac{dv}{dt} \leq 0,$$

with equality if and only if

$$N(t) = \frac{\pi + \pi_i - \mu I^*}{\mu}.$$

Thus, $\frac{dv}{dt} < 0$, indicating that v is a Lyapunov function and the endemic equilibrium point E^* is globally asymptotically stable. □

8. Global stability of disease free equilibrium point

The model system (1) may be expressed as follows:

$$\begin{cases} \frac{dP}{dt} = F(P,\ Q), \\ \\ \frac{dQ}{dt} = F(P,\ 0),\ G(P,\ 0). \end{cases}$$

In this case, the numbers of uninfected compartments ($P \in R^m$), infected compartments ($Q \in R^n$), and disease-free equilibrium points ($E^0 = (P^0,\ 0)$) are shown. In order to ensure the grantee's global asymptotic stability of DFE, the following conditions $(H1)$ and $(H2)$ need to be met. $H1 =$ For$\frac{dP}{dt} = F(P,\ 0),\ P^0$, is globally asymptotically stable, $H2 =$ For $G(P,\ Q) = XQ - G^-(P,\ Q),\ G^-(P,\ Q) \geq 0$. For $P,\ Q \in \Omega$, where $XA_1(P^0,\ 0)$ is the Metzler Matrix thanks to its non-negative off-diagonal components of X, and Ω denotes the region where the epidemiologically significant rabies model system (1) is supplied.

Consequently, if the system meets the aforementioned requirement $(H1)$ and $(H2)$, Hence the following theorem is true.

Theorem 4 The diseases free equilibrium point $E_0 = (P^0,\ 0)$ is unstable otherwise and globally asymptotically stable if $R_e < 1$.

Proof. The model system for rabies (1) may be expressed as; $P = (S,\ V,\ R) = (E,\ I)$ and

$$E_0 = \left(\frac{\phi\mu(\theta + \phi + \mu) + (\theta\tau\phi)}{(\theta + \mu)\mu(\theta + \tau + \mu)},\quad 0,\quad \frac{\pi\theta}{\mu(\theta + \tau + \mu)},\quad 0,\quad 0 \right).$$

Now, we have

$$\frac{dp}{dt} = \begin{pmatrix} \pi + \eta R + \tau V - (\beta I + \theta + \mu)S, \\ \alpha_1 E + \theta S - (\tau + \mu + (1-\varepsilon)\beta I)V, \\ \alpha_2 E - (\mu + \eta)R. \end{pmatrix}$$

At disease free equilibrium

$$\frac{dP}{dt} = F(P^0,\ 0) = \begin{pmatrix} \phi + \tau\dfrac{\pi\theta}{\mu(\theta+\tau+\mu)} - (\theta+\mu)\dfrac{\phi\mu(\theta+\phi+\mu)+(\theta\tau\phi)}{(\theta+\mu)\mu(\theta+\tau+\mu)} \\ \theta\dfrac{\phi\mu(\theta+\phi+\mu)+(\theta\tau\phi)}{(\theta+\mu)\mu(\theta+\tau+\mu)} - (\tau+\mu)\dfrac{\pi\theta}{\mu(\theta+\tau+\mu)} \\ 0 \end{pmatrix} \tag{3}$$

$F(P^0,\ 0)$ possesses a distinct equilibrium point. $P^0 = \left(\dfrac{\phi\mu(\theta+\phi+\mu)+(\theta\tau\phi)}{(\theta+\mu)\mu(\theta+\tau+\mu)},\ \dfrac{\pi\theta}{\mu(\theta+\tau+\mu)}\right)$, This is asymptotically stable worldwide. Because of this, $(H1)$ holds true. Regarding the second conation $(H2)$

$$G(P,\ Q) = \begin{pmatrix} \beta SI + (1-\varepsilon)\beta VI - (\alpha_1+\alpha_2+\delta+\mu)E, \\ \pi_i + \delta E - (\mu+\mu_1)I \end{pmatrix} \tag{4}$$

Then we get

$$X = A_1(P^0,\ 0) = \begin{pmatrix} -(\alpha_1+\alpha_2+\delta+\mu) & \beta S^* + (1-\varepsilon)\beta V^*, \\ \delta & -(\mu+\mu_1) \end{pmatrix} \tag{5}$$

.

Now, it is clear that because the diagonal elements of the matrix are non-negative. Hence $\hat{G}(P,\ Q) = XA - G(P,\ Q)$ equals to

$$\hat{G}(P,\ Q) = \begin{pmatrix} -(\alpha_1+\alpha_2+\delta+\mu) & \beta S^* + (1-\varepsilon)\beta V^* \\ \delta & -(\mu+\mu_1) \end{pmatrix} \begin{pmatrix} E \\ I \end{pmatrix} \begin{pmatrix} \beta SI + (1-\varepsilon)\beta VI - (\alpha_1+\alpha_2+\delta+\mu)E \\ \pi_i + \delta E - (\mu+\mu_1)I \end{pmatrix} \tag{6}$$

$$\hat{G}(P,\ Q) = \begin{pmatrix} \beta S^0 + (1-\varepsilon)\beta V^0 - (\beta S + (1-\varepsilon)\beta V) \\ 0 \end{pmatrix} \Rightarrow \hat{G}(P,\ Q) = \begin{pmatrix} \beta(S^0 - S) + (1-\varepsilon)\beta(V^0 - V) \\ 0 \end{pmatrix} \tag{7}$$

Given that it is evident that $S^0 > S$ and $V^0 > V$, it follows that $\hat{G}(P,\ Q) \neq 0$, and $P^0 = P^0 = \left(\dfrac{\phi\mu(\theta+\phi+\mu)+(\theta\tau\phi)}{(\theta+\mu)\mu(\theta+\tau+\mu)},\right.$ $\left.\dfrac{\pi\theta}{\mu(\theta+\tau+\mu)}\right)$, is globally asymptotically stable.

9. Bifurcation

In mathematical models, bifurcation describes situations in which little adjustments to the parameters result in notable changes in the behavior of the system. It makes clear the pivotal moments at when the system's dynamics radically shift, helping us to comprehend how systems change and adapt to different circumstances. In order to determine β^*, we must set $R_0 = 1$ in order to verify the bifurcation of our model [22]. The jacobian matrix of the model (1) is given as

$$J^*_\beta = \begin{bmatrix} -(\mu+\theta) & 0 & \beta^* S^* & \tau & \eta \\ 0 & -(\mu+\alpha_1+\alpha_2+\delta) & \beta^* S^* & 0 & 0 \\ 0 & \delta & -(\mu+\mu_1-\alpha_1) & 0 & 0 \\ \theta & \alpha_1 & 0 & -(\mu+\tau) & 0 \\ 0 & \alpha_2 & 0 & 0 & -(\mu+\eta) \end{bmatrix}$$

After some steps of the calculation we have determined the eigenvalue of $J\beta^*$

$$\gamma_1 = -(\mu+\theta),\ \gamma_2 = -(\mu+\mu_1-\alpha_1),\ \gamma_3 = -(\mu+\alpha_1-\alpha_2+\delta),\ \gamma_4 = \mu+\tau, \gamma_5 = \mu+\eta.$$

It demonstrates that every eigenvalue is a negative real point. In this case, the dynamics of the model may be examined using the theorem Castillo, Chavez, and Song [22] to demonstrate that the eigenvector of $J\beta^*$

In this section we will find the right and left eigenvectors, then on the base of these eigenvector, we will describe that what type bifurcation exist

$$J|0|(\beta^*)K = 0,$$

$$J\beta^* = \begin{bmatrix} -(\mu+\theta) & 0 & \beta^* S^* & \tau & \eta \\ 0 & -(\mu+\alpha_1+\alpha_2+\delta) & \beta^* S^* & 0 & 0 \\ 0 & \delta & -(\mu+\mu_1) & 0 & 0 \\ \theta & \alpha_1 & 0 & -(\mu+\tau) & 0 \\ 0 & \alpha_2 & 0 & 0 & -(\mu+\eta) \end{bmatrix} \begin{bmatrix} K_1 \\ K_2 \\ K_3 \\ K_4 \\ K_5 \end{bmatrix} = \begin{bmatrix} 0 \\ 0 \\ 0 \\ 0 \\ 0 \end{bmatrix}$$

$$-K_1\mu - K_{\neg 1}(\mu+\theta) + \beta^* S^* K_3 + \tau K_4 + \eta K_5 = 0 \tag{8}$$

$$-K_2\mu - K_{\neg 2}(\mu+\alpha_1+\alpha_2+\delta) + \beta^* S^* K_3 = 0 \tag{9}$$

$$K_2\delta - K_3(\mu+\mu_{\neg\neg 1}) = 0 \tag{10}$$

$$\theta K_1 + \alpha_1 K_2 - K_4(\mu+\tau) = 0 \tag{11}$$

$$\alpha_2 K_2 - K_5(\mu+\eta) = 0 \tag{12}$$

The left eigenvector associated with the zero eigenvalue may now be found by using the formula $VJ|0|(\beta^*) = 0$.

$$\begin{cases} -(\mu+\theta)V_1+\theta V_4=0 \\ \\ -(\mu+\alpha_1+\alpha_2+\delta)V_2-\delta V_3+\alpha_1 V_4+\alpha_2 V_5=0 \\ \\ V_1\beta^* S^*+V_2\beta^* S^*-(\mu+\mu_1)V_3=0 \\ \\ V_1\tau-\theta(\mu+\tau)V_4=0 \\ \\ \eta V_1-V_5(\mu+\eta)=0 \end{cases} \tag{13}$$

After solution the above system of equation we get the following result $V_1=V_4=V_5=0$.

We can write in model (1) the form $\frac{dg}{dt}=g(x)$ with $g=\left(g_1,\ g_2,\ g_3,\ g_4,\ g_5\right)^{\mathsf{T}}$ as follows by setting $S=y_1,\ E=y_2,\ I=y_3,\ V=y_4,\ R=y_5$.

$$\begin{aligned} g(y)=g_1&=\pi+\tau y_4+\eta y_5-(\beta y_3+\mu+\theta)y_1, \\ g(y)=g_2&=\beta y_1 y_3+(1-\varepsilon)\beta y_4 y_3-(\mu+\alpha_1+\alpha_2+\delta)y_2, \\ g(y)=g_3&=\delta y_2+\pi_i-(\mu+\mu_1)y_3, \\ g(y)=g_4&=\theta y_1+\alpha_1 y_2-(\mu+\tau+(1-\varepsilon)\beta y_3)y_4, \\ g(y)=g_5&=\alpha_2 y_2-(\mu+\eta)y_5. \end{aligned} \tag{14}$$

We get the function of g by using the value of the left eigenvector V. We only pick g_2 and g_3, and we then determine the partial derivative of their second order in the following manner.

$$\begin{cases} g_2(y)=\beta y_1 y_3+(1-\beta)\beta y_4 y_3-(\mu+\alpha_1+\alpha_2+\delta)y_2, \\ \\ g_3(y)=\eta y_2+\pi_i-(\mu+\mu_1)y_3. \end{cases} \tag{15}$$

$$\frac{\partial^2 g_2}{\partial y_1 \partial y_j}(E_0,\ \beta^*) = 0 \quad \text{for } j = 1,\ 2,\ 4,\ 5$$

$$\frac{\partial^2 g_2}{\partial y_1 \partial y_3}(E_0,\ \beta^*) = \beta^* \quad \text{for } J = 3$$

$$\frac{\partial^2 g_2}{\partial y_2 \partial y_j}(E_0,\ \beta^*) = 0 \quad \text{for } J = 1,\ 2,\ 3,\ 4,\ 5$$

$$\frac{\partial^2 g_2}{\partial y_3 \partial y_j}(E_0,\ \beta^*) = 0 \quad \text{for } J = 2,\ 3,\ 4.$$

$$\frac{\partial^2 g_2}{\partial y_3 \partial y_j}(E_0,\ \beta^*) = \beta^*(1-\varepsilon) \quad \text{for } J = 1,\ 4$$

$$\frac{\partial^2 g_2}{\partial y_4 \partial y_j}(E_0,\ \beta^*) = 0 \quad \text{for } J = 1,\ 2,\ 4,\ 5$$

$$\frac{\partial^2 g_2}{\partial y_4 \partial y_j}(E_0,\ \beta^*) = \beta^*(1-\varepsilon) \quad \text{for } J = 3$$

$$\frac{\partial^2 g_2}{\partial y_5 \partial y_j}(E_0,\ \beta^*) = 0 \quad \text{for } J = 1,\ 2,\ 3,\ 4,\ 5$$

$$\frac{\partial^2 g_3}{\partial y_i \partial y_j}(E_0,\ \beta^*) = 0 \quad \text{for } J = 1,\ 2,\ 3,\ 4,\ 5$$

$$\frac{\partial^2 g_3}{\partial y_i \partial \beta^*}(E_0,\ \beta^*) = 0 \quad \text{for } j = i = 1,\ 2,\ 3,\ 4,\ 5$$

We get the bifurcation coefficients, a and b, as, taking into consideration the eigenvalues on the left and right.

$$a = \sum_{k,i=j=1}^{5} V_k K_i K_j \frac{\partial^2 g_k}{\partial y_i \partial \beta^*} \tag{16}$$

$$b = \sum_{k,i=j=1}^{5} V_k K_j \frac{\partial^2 g_k}{\partial y_i \partial \beta^*} \tag{17}$$

It can be shown from the foregoing relation (10) and (11) that only V_2, V_3, are non-zero.

$$a = V_2 \sum_{k,i=j=1}^{5} K_i K_j \frac{\partial^2 g_2}{\partial y_i \partial \beta^*} + V_2 \sum_{k,i=j=1}^{5} K_i K_j \frac{\partial^2 g_3}{\partial y_i \partial \beta^*}$$

$$b = V_2 \sum_{k,i=j=1}^{5} K_j \frac{\partial^2 g_2}{\partial y_i \partial \beta^*} + V_3 \sum_{k,i=j=1}^{5} K_j \frac{\partial^2 g_3}{\partial y_i \partial \beta^*}$$

to find the value of (a) we exclusive taken into account the non-zero order partial derivative of $g_2,\ g_3$, all $\frac{\partial g_2}{\partial y_i \partial y_j}$ and zero except, Similarly,

$$\frac{\partial g_i}{\partial y_i \partial y_j} = 0,$$

therefore, the above equation

$$a = V_2 \sum_{k,i=j=1}^{5} K_i K_j \frac{\partial^2 g_2}{\partial y_i \partial \beta^*} + V_3 \sum_{k,i=j=1}^{5} K_i K_j \frac{\partial^2 g_3}{\partial y_i \partial \beta^*} \tag{18}$$

$$a = V_2 \sum_{k,i=j=1}^{5} K_i K_j \frac{\partial^2 g_2}{\partial y_i \partial \beta^*} \tag{19}$$

$$a = v_2 \left(\frac{\beta^* S^* K_3 + \tau K_4 + \eta K_5}{(\mu + \theta)} \cdot \frac{K_2 \delta}{(\mu + \mu_1)} \beta^* (1 - \varepsilon) + \frac{\theta K_1 + \alpha_1 K_2}{(\mu + \tau)} \cdot \frac{K_2 \delta}{(\mu + \mu_1)} \beta^* (1 - \varepsilon) \right) > 0$$

$$b = V_2 K_1 \beta + V_3 \sum_{k,i=j=1}^{5} K_j(0)$$

$$b = V_2 \frac{\beta^* S^* K_3 + \tau K_4 + \eta K_5}{(\mu + \theta)} \beta > 0$$

According to the hypothesis, the 1 model exhibits a phenomenon of backward bifurcation at $R_0 = 1$, since $a > 0$ and $b > 0$. several equilibrium points coexisting. The initial number of afflicted people is also very important.

Common prerequisites for curing sickness, such creating $R_0 < 1$, will not function in such a reason.

10. Numerical simulations

The MATLAB 2018a software with ODE45 solver, which combines 4th-order and 5th-order Runge-Kutta (RK5) methods, was used to perform the numerical simulation in this section. Its ability to accurately represent the dynamics of the rabies transmission model has been demonstrated. The starting parameters that are used in the simulation are: $S = 500,\ V = 0,\ E = 100,\ I = 100$, and $R = 0$. The initial conditions are chosen at random to influence the model's

behavior in a specific manner. Figure 5 depicts the population trends of the rabies population. Figures 6, 7, 8, 9, and 10 provide graphical representations of the susceptible, exposed, infected, vaccinated, and recovered classes, respectively.

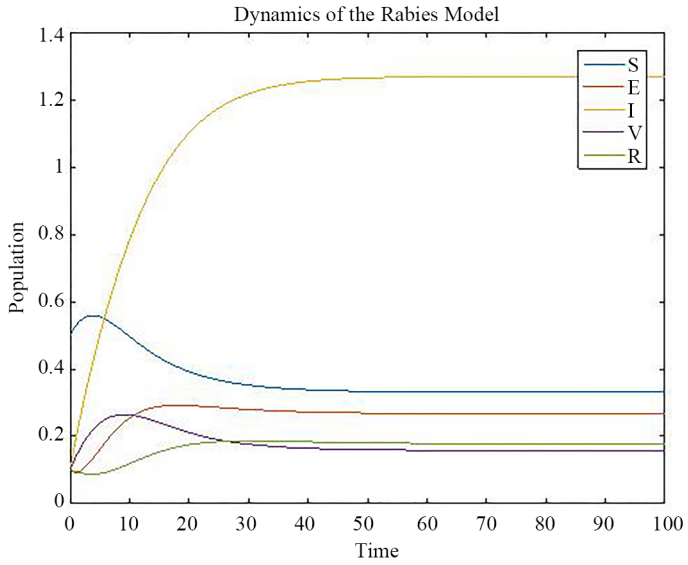

Figure 5. Animal population evolution over time

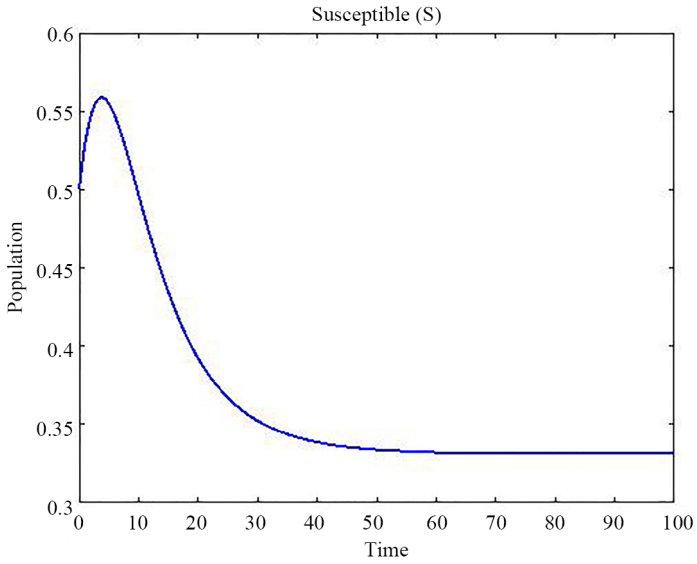

Figure 6. Susceptible animal population

The findings show that the number of animals that are sensitive rapidly declines in the early years. The two main causes of this decline are as follows: the first is the rise in vaccination administration at a steady pace of 0.1 (vaccine effectiveness of $\alpha_1 = 0.1$). By immunizing vulnerable animals against rabies, this strategy seeks to reduce the animals' vulnerability to the illness. Second, the infection contracted via interacting with diseased animals also plays a role in the decline of animals that are vulnerable. Animals that are vulnerable to infection are exposed to the virus when they interact with infected people, which lowers their susceptibility. In keeping with one health approach put forth by

Acharya et al. [23], the dynamics of these processes shown graphically offers insightful information about the early effectsof immunization and illness dissemination on the rabies populace. It also emphasizes the significance of efficient immunization tactics as well as the necessity of controlling infection transmission in order to effectively treat rabies.

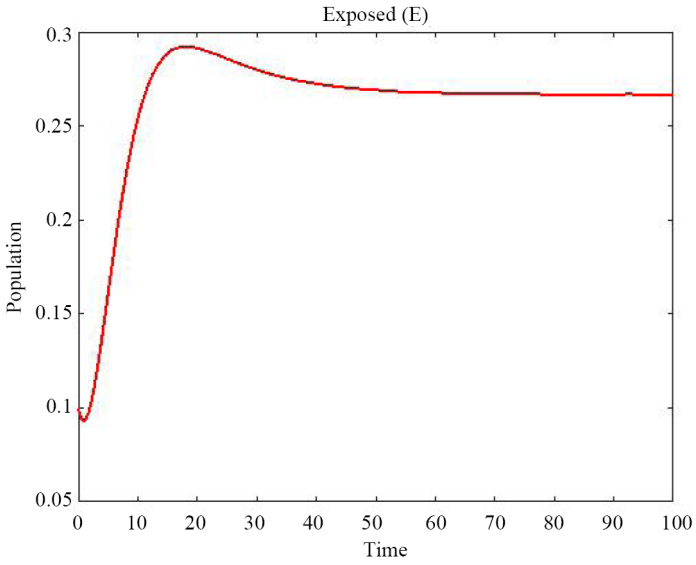

Figure 7. Exposed population

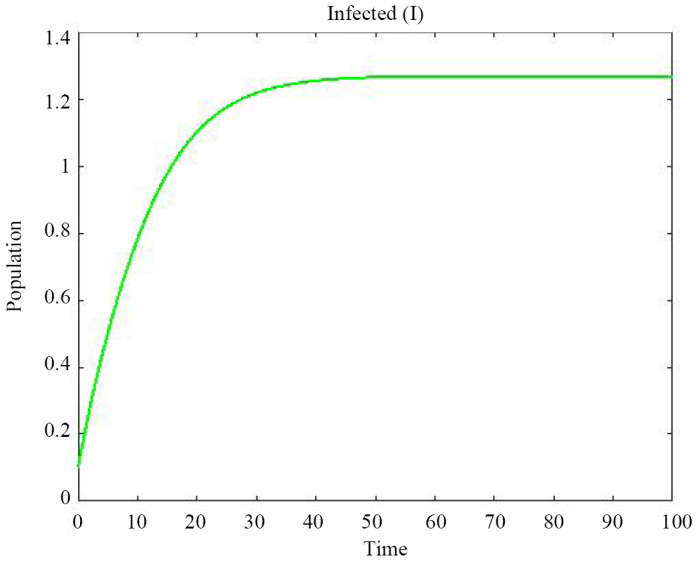

Figure 8. Infected animal population

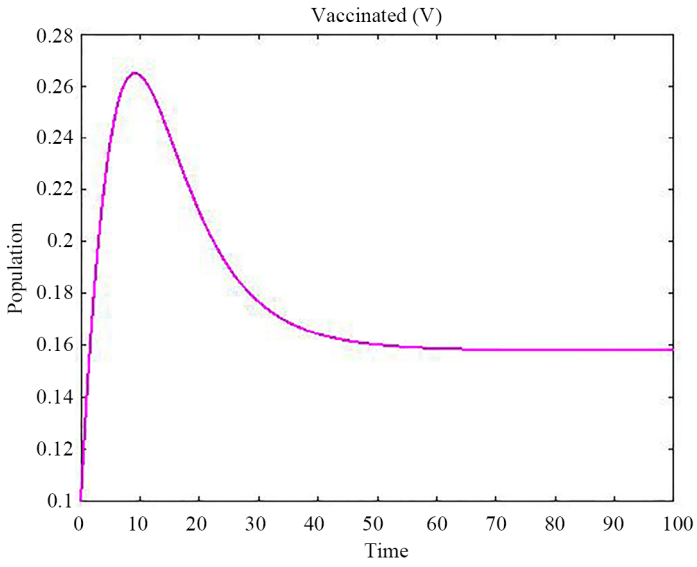

Figure 9. Vaccinated animal population

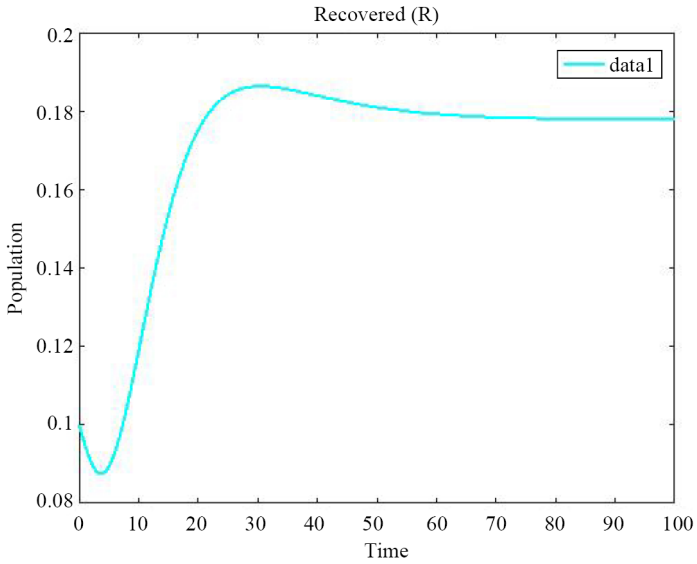

Figure 10. Recovered population

11. Simulation of the impact of changing parameter values on the model's parameters

The purpose of the parameter value variation in this part was to examine the behavior of the state variables in response to the parameter value change. The simulation is performed with respect to the most sensitive factors, and Figure 11 displays the outcomes. It is clear from Figure 11 that when the vaccine is administered successfully, there is a decrease in the number of sick animals due to the rise in vaccination efficiency.

A growing proportion of immunized animals acquire immunity against rabies, making them less susceptible to infection, as vaccination efficiency increases. Over time, this causes the number of affected animals to decrease. The graph highlights how crucial vaccination effectiveness is in stopping the spread of rabies.

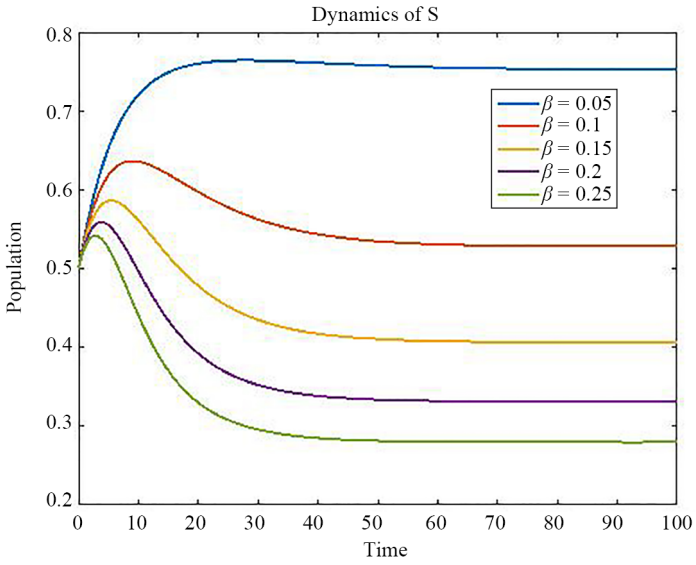

Figure 11. Effect of β of susceptible animal population

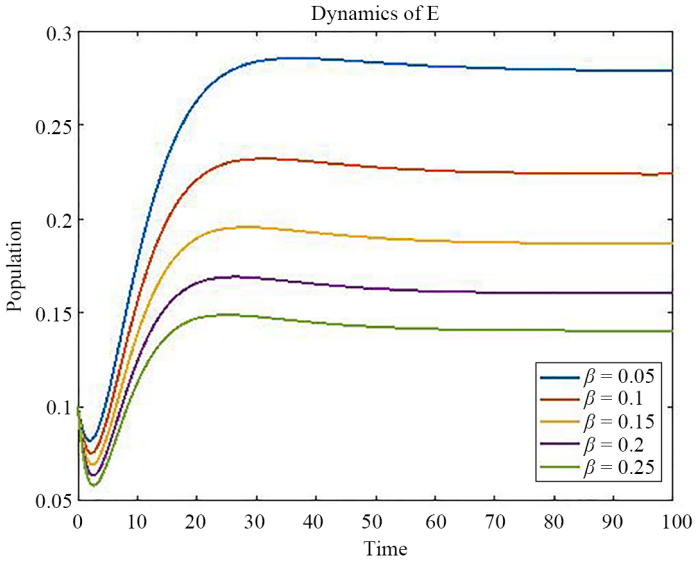

Figure 12. Effect of β of exposed animal population

Stronger protection is provided by a more potent vaccination, which also helps to reduce the overall number of sick animals by preventing the disease's spread. These results highlight the need of ongoing efforts to create and use vaccines with high rates of effectiveness as a vital weapon in the fight against rabies and safeguarding public health.

It is clear from Figure 12 that a rise in vaccination efficiency β causes a drop in the quantity of animals exposed. An increasing proportion of vaccinated animals acquire immunity to rabies, decreasing the probability of their coming into

contact with the virus, as the vaccine grows more effective. The graph effectively depicts how the dynamics of exposed animals within the population are impacted by vaccination effectiveness.

More people who receive vaccinations are protected, which results in fewer animals being exposed to the illness, when the efficacy of the vaccination is higher. This result highlights how important it is to increase vaccination effectiveness in preventing rabies from spreading and reducing the number of animals that are at danger of infection. These findings demonstrate the critical role that vaccinations play in lowering the risk of contracting rabies and reinforce the significance of ongoing research and development initiatives to improve vaccine effectiveness as a cornerstone tactic in the prevention and control of rabies.

11.1 *Effects of intervention on infected rabies animals*

A simulation of the model was performed. in this part both with and without intervention, and Figure 8 presents a summary of the outcomes. It is clear from Figure 8 that illness infection rates are high in the absence of vaccine application. However, rabies disease infections tend to decline dramatically with the vaccine being implemented at a steady pace of $\theta = 0.1$ (with vaccination efficiency of $\varepsilon = 0.94$).

Because of this, the prevalence of the sickness has been gradually dropping over time, and the infection is expected to finally go extinct in the population. This finding highlights the vital role that vaccination plays in managing and preventing the spread of rabies, ultimately resulting in the disease's eradication from the general population. The work of Lavan et al. [10] supports the graphical approach, which clearly visualizes the beneficial effect of immunization on the rabies infection's dynamics and emphasizes the significance immunization campaigns in the field of public health policies.

11.2 *Simulation of the model's response to changing infectious immigrant parameter values*

The consequences of a rise in the quantity of infectious immigrants $(\pi_i \times I)$ on various demographic groups are well displayed in Figure 13, 14, and 15. The increasing number of infectious immigrants has different effects on communities that are susceptible, immunized, and recoverable. More specifically, Figure 12 shows that the number of vulnerable individuals decreases as infectious immigrants rise.

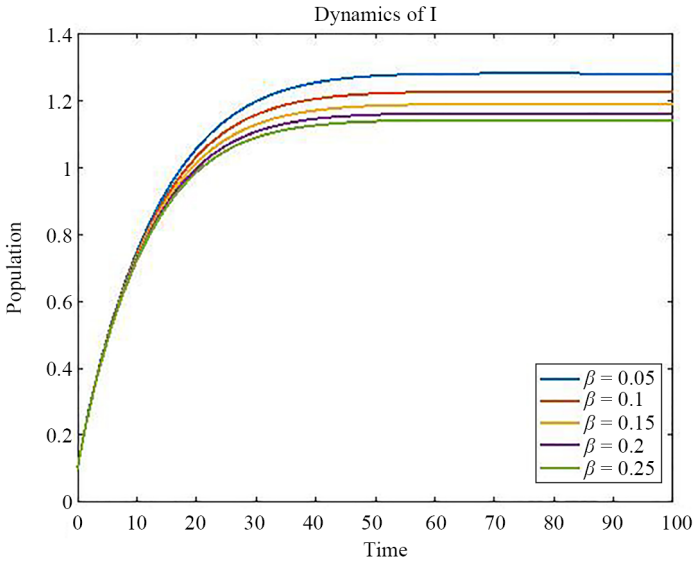

Figure 13. Effect of β of infected animal population

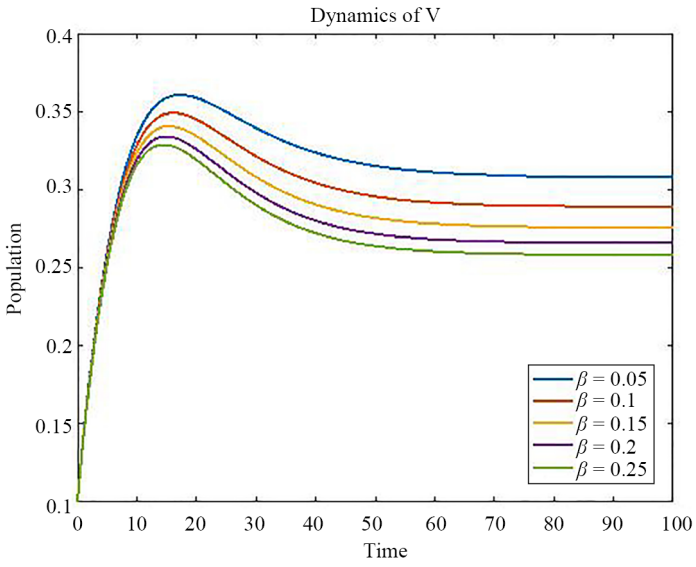

Figure 14. Effect of β of vaccinated animal population

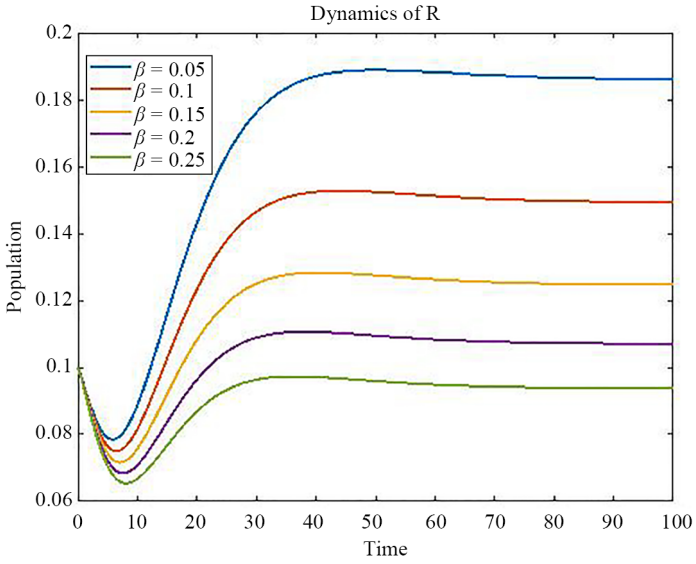

Figure 15. Effect of β of recovered animal population

This is to be expected as the entry of infected people from outside sources increases the chance that susceptible people may contract the disease, which eventually reduces the susceptible population. Figure 9 illustrates how an increase in infectious Immigration lowers the proportion of vaccinated animals. This result implies that, in spite of vaccination campaigns, people may expose vaccinated animals to viruses, which might cause an increase in the population's proportion of vaccinated animals. However, Figure 14 clearly shows that a rise in infectious immigrants leads to a fall in the number of recovered persons. This suggests that reintroducing diseased animals from outside sources might result in reinfections, which would impede the healing process and lower the total number of animals that are recovered.

On the other hand, it is noted that the effects of infectious immigrants on populations that are exposed and affected varies. As predicted, the number of sick animals rises in Figure 6 in response to an increase of infectious immigrants. Parallel to this, Figure 7 shows that when infectious immigrants grow, more animals get exposed since they can spread the virus to other vulnerable animals, leading to an increase in the number of exposed animals. These results demonstrate how important it is to manage the dynamics of the rabies population by limiting the number of contagious immigrants entering the nation.

According to Chen et al. [18] and Blackwood et al. [24], preventing the import of infected animals from outside sources can help limit the disease's spread and protect susceptible and vaccinated persons from possible infections. These findings have substantial implications for the design and execution of initiatives aimed at lowering the prevalence of the illness and emphasize the need of border security measures in rabies-affected regions.

12. Conclusion

To comprehend the transmission dynamics of animal rabies, we formulated a mathematical model that considers affective variables like the incursion of infected individuals from other areas and used the impact of vaccination as a preventive measure. The reproduction number (R_0) has been calculated using the well-known next-generation matrix (NGM) method. Through the application of the Routh-Hurwitz criterion, we have identified a Disease-Free Equilibrium (DFE) point and recognized its stability condition as R_0 being less than 1 for stability and greater than 1 for instability. Moreover, we have confirmed the global stability of the DFE by analyzing it with a quadratic Lyapunov function. The central manifold theory is used for Bifurcation analysis, and the normalized forward sensitivity index technique is used for sensitivity of model parameters and variation in R_0. Numerical simulations have been carried out using the MATLAB program. The produced research has shown that an increase in vaccination rates and a decrease in the number of infected immigrants entering a population can excellently slow down the transmission of rabies. These results emphasize the significance of controlling the influx of infectious immigrants as a strategy to significantly manage the spread of rabies. The implications of these results are important for the development and implementation of strategies aimed at reducing the occurrence of rabies, underlining the role of a successful vaccination campaign in limiting the transmission of the disease. Sensitivity analysis has indicated that the transmission rate (β) has the most significant effect on the spread of rabies, while the efficacy of vaccination (ε) plays a vital role in reducing the occurrence of the disease. Our simulation study, carried out using MATLAB, has established that adjusting rabies transmission can be achieved by controlling the number of infectious immigrants and increasing vaccination rates. These results advocate that in order to effectively control rabies, it is important to assume measures that focus on reducing the entry of diseased individuals into a population and boosting the percentage of individuals vaccinated against rabies. However, further research is essential to address the limitations of our model, including the simplifications and assumptions, which could possibly affect its accuracy.

Finally, we provided graphs for understanding the dynamics of rabies transmission and evaluating the impact of various parameters on the epidemic's progression. They illustrate the changes in susceptible, exposed, infected, vaccinated, and recovered populations over time, highlighting the effects of different transmission rates and control measures. These insights are crucial for identifying equilibrium states, validating and improving mathematical models, and supporting effective policy and decision-making for rabies control.

Acknowledgement

All authors have been agreed to submit this version.

Conflict of interest

The authors declare there is no conflict of interest at any point with reference to research findings.

References

[1] Lempp C, Jungwirth N, Grilo ML, Reckendorf A, Ulrich A, Siebert U. Pathological findings in the red fox (vulpes vulpes), stone marten (martes foina) and raccoon dog (nyctereutes procyonoides), with special emphasis on infectious and zoonotic agents in Northern Germany. *PLoS One*. 2017; 12(4): 0175469.

[2] Fisher CR, Streicker DG, Schnell MJ. The spread and evolution of rabies virus: Conquering new frontiers. *Nature Reviews Microbiology*. 2018; 16(4): 241-255.

[3] Hankins DG, Rosekrans JA. Overview, prevention, and treatment of rabies. *Mayo Clinic Proceedings*. 2004; 79(5): 671-676.

[4] Demirci E. A new mathematical approach for rabies endemy. *Applied Mathematics and Information Sciences*. 2014; 8(2): 59-67.

[5] Guedri K, Ramzan Y, Awan AU, Fadhl BM, Oreijah M. Modeling transmission patterns and optimal control through nanotechnology: A case study of malaria causing brain disabilities. *Journal of Disability Research*. 2024; 3(1): 20230061.

[6] Gilani SQ, Syed T, Umair M, Marques O. Skin cancer classification using deep spiking neural network. *Journal of Digital Imaging*. 2023; 36(3): 1137-1147.

[7] Balaha HM, Hassan AES. Skin cancer diagnosis based on deep transfer learning and sparrow search algorithm. *Neural Computing and Applications*. 2023; 35(1): 815-853.

[8] Savov P, Jatowt A, Nielek R. Identifying breakthrough scientific papers. *Information Processing Management System*. 2020; 57(2): 102168.

[9] Kalathil N, Byrnes JJ, Randazzese L, Hartnett P D, Freyman CA. Application of text analytics to extract and analyze material application pairs from a large scientific corpus. *Frontiers in Research Metrics and Analytics*. 2018; 2: 1-13. Available from: https://doi.org/10.3389/frma.2017.00015.

[10] Lavan RP, King AIM, Sutton DJ, Tunceli K. Rationale and support for a One Health program for canine vaccination as the most cost-effective means of controlling zoonotic rabies in endemic settings. *Vaccine*. 2017; 35(3): 1668-1674.

[11] Blei DM, Ng AY, Jordan MI. Latent dirichlet allocation. *Journal of Machine Learning Research*. 2003; 3: 993-1022.

[12] Gan J, Qi Y. Selection of the optimal number of topics for LDA topic model taking patent policy analysis as an example. *Entropy*. 2021; 23(10): 1301.

[13] Cao J, Xia T, Zhang Y, Tang S. A density-based method for adaptive LDA model selection. *Neurocomputing*. 2009; 72(7-9): 1775-1781.

[14] Piot P, Sureau P, Breman G, Heymann D, Kintoki V, Masamba M, et al. Clinical aspects of ebola virus infection in yambuku area, Zaire 1976. *African Journal of Infectious Diseases*. 1978; 210(96): 34-51.

[15] Guedri K, Ramzan Y, Awan AU, Fadhl BM, Ali B, Oreijah M. Rabies-related brain disorders: Transmission dynamics and epidemic management via educational campaigns and application of nanotechnology. *The European Physical Journal Plus*. 2024; 139(1): 1-16.

[16] Lushasi K, Hayes S, Ferguson EA, Changalucha J, Cleaveland S, Govella N, et al. Reservoir dynamics of rabies in south-east tanzania and the roles of cross species transmission and domestic dog vaccination. *Journal of Applied Ecology*. 2021; 58(11): 2673-2685.

[17] Ramzan Y, Awan AU, Ozair M, Hussain T, Mahat R. Innovative strategies for Lassa fever epidemic control: A groundbreaking study. *American Institute of Mathematical Sciences Mathematics*. 2023; 8(12): 30790-30812.

[18] Chen J, Zou L, Jin Z, Ruan S. Modeling the geographic spread of rabies in China. *PLoS Neglected Tropical Diseases*. 2015; 9(5): e0003772.

[19] Ahmed I, Tariboon J, Muhammad M, Ibrahim MJ. A mathematical and sensitivity analysis of an HIV/AIDS infection model. *International Journal of Mathematics and Computer in Engineering*. 2025; 3(1): 35-46.

[20] Simon C, Davidsen K, Hansen C, Seymour E, Barnkob MB, Olsen LR. BioReader: A text mining tool for performing classification of biomedical literature. *BMC Bioinformatics*. 2019; 19(Suppl 13): 165-170.

[21] Vargas-De-León C. Constructions of Lyapunov functions for classic SIS, SIR and SIRS epidemic models with variable population size. *Foro-Red-Mat: Revista Electronica De Contenido Matematico*. 2009; 26(5): 1-12.

[22] Kotola BS, Teklu S, Abebaw YF. Bifurcation and optimal control analysis of HIV/AIDS and COVID-19 co-infection model with numerical simulation. *Plos One*. 2023; 18(5): e0284759.

[23] Acharya KP, Acharya N, Phuyal S, Upadhyaya MS, Lasee S. One-health approach: A best possible way to control rabies. *One Health*. 2020; 10: 100161. Available from: https://doi.org/10.1016/j.onehlt.2020.100161.

[24] Blackwood JC, Streicker DG, Altizer S, Rohani P. Resolving the roles of immunity, pathogenesis, and immigration for rabies persistence in vampire bats. *Proceedings of the National Academy of Sciences*. 2013; 110(51): 20837-20842.